PCCP

Rotational spectroscopy of *C*-cyanophosphaethyne, NCCP, in states of multiple vibrational excitation†

L. Bizzocchi,*[a] C. Degli Esposti,[a] S. Thorwirth,[b] H. S. P. Müller,[b] F. Lewen[b] and G. Winnewisser[b]

[a] *Dipartimento di Chimica "G. Ciamician", Università di Bologna, via F. Selmi 2, 40126 Bologna, Italy. E-mail: bizzo@ciam.unibo.it*

[b] *I. Physikalisches Institut, Universität zu Köln, Zülpicherstraße 77, 50937 Cologne, Germany*

Received 26th March 2001, Accepted 25th June 2001
First published as an Advance Article on the web 1st August 2001

The rotational spectrum of the unstable NCCP molecule has been investigated in the millimetre-wave region for all the levels of multiple vibrational excitation below 1200 cm^{-1}. More than 600 rotational transitions in the J range from 19 to 39 have been measured and assigned to 13 new vibrational states derived from excitation of the two bending modes v_4 and v_5 and of the low-energy stretching mode v_3. Transitions up to $J = 141$ have been included in the fit for $v_3 = 1$ yielding a precise value for the sextic centrifugal distortion constant. Vibrational and rotational l-type resonance effects have been taken into account in the analyses of the observed spectra together with the anharmonic interactions which originate from the normal coordinate force constants k_{345}, k_{344}, k_{35555} and k_{34555}. The simultaneous analyses of the rotational spectra of the interacting levels have yielded sets of spectroscopic constants with unambiguous physical meaning, including the unperturbed value of the α_3 vibration–rotation coupling constant, and the $x_{L(44)}$, $x_{L(55)}$ and $x_{L(45)}$ anharmonic constants.

1 Introduction

The linear phosphaalkyne NCCP (*C*-cyanophosphaethyne) is a moderately unstable compound which was originally produced by Kroto's group by means of a gas-phase high-temperature reaction between cyanogen azide, NCN_3, and phosphaethyne, HCP.[1] A Stark-modulation microwave spectrometer was employed to detect the new molecule and a few ground-state rotational transitions were recorded in the centimetre-wave (cm-wave) region for the most abundant isotopomer.

After that first investigation, NCCP was recently the object of a joint theoretical–experimental study, in which an *ab initio* cubic force field, obtained from high level CCSD(T) calculations using the cc-pVQZ basis set, provided accurate predictions for the ground-state rotational constants of the ^{13}C- and ^{15}N-substituted species, whose millimetre-wave (mm-wave) rotational spectra were then detected in natural abundance, thus allowing the first experimental determination of the structural parameters of this molecule.[2] The theoretically computed cubic force field also provided very precise estimates of the α_τ vibration–rotation coupling constants, through which the mm-wave spectra of the most abundant isotopomer in the vibrationally excited states $v_2 = 1$ (C≡P stretch, Σ symmetry), $v_3 = 1$ (C–C stretch, Σ symmetry), $v_4 = 1$ (CCN bend, Π symmetry) and $v_5 = 1$ (CCP bend, Π symmetry) could be identified and analysed. Because in the present work only vibrational states excited in v_3, v_4 and v_5 have been investigated, the contracted notation (v_3, v_4, v_5) is used throughout the paper to designate states. The rotational spectrum of the (1, 0, 0) state was found to be perturbed by an anharmonic resonance with the nearby (0, 1, 1) combination state, but no detailed analysis of the detected interaction was performed.

In a subsequent work, the study of the rotational spectrum of NCCP has been extended to the submm-wave region (from 490 to 820 GHz) reaching J values up to 150.[3] Improved spectroscopic parameters and novel values of the sextic centrifugal distortion constants were obtained for the ground state of the normal, ^{13}C- and ^{15}N-substituted species, and for the (0, 1, 0) and (0, 0, 1) excited states of the most abundant isotopomer.

The present paper reports the identifications and the analyses of the rotational spectra for the 13 overtone and combination states of NCCP which lie below 1200 cm^{-1}, namely the bending overtone states (0, 2, 0), (0, 0, 2), (0, 0, 3), (0, 0, 4), (0, 0, 5), and (0, 0, 6), the bend–bend combination states (0, 1, 1), (0, 1, 2), (0, 1, 3), and (0, 2, 1), and the stretch–bend combination states (1, 0, 1), (1, 0, 2), and (1, 1, 0). Most of the studied vibrational states involve multiple excitation of bending modes, and thus vibrational and rotational l-type resonance effects have been taken into account to analyse properly the observed spectra. In addition, we have observed that nearly all the states investigated are perturbed by anharmonic interactions, the only exceptions being (0, 0, 2) and (0, 0, 3). Basically the same resonances which perturb the excited state rotational spectra of the isoelectronic HC_3P molecule[4] are also present in NCCP. As already pointed out in ref. 2, the (1, 0, 0) stretching state is strongly coupled to the bending combination state (0, 1, 1) through the k_{345} normal coordinate cubic force constant, but weaker interactions do also exist between (1, 0, 0) and (0, 2, 0) (through k_{344}), and between (1, 0, 0) and (0, 0, 4) (through k_{35555} and related perturbation products of the $\tilde{H}_{50}$ transformed Hamiltonian[5]). Analogously to HC_3P, the main resonance system of NCCP is therefore a tetrad which includes the (1, 0, 0), (0, 1, 1), (0, 2, 0) and (0, 0, 4) vibrational states. Two further polyads have been also investigated in the present study, corresponding to the addition of one or two quanta of the lowest bending v_5 to the levels of the first resonance system. In the course of these latter analyses, the high-order anharmonic interaction produced by k_{34555} and related terms of $\tilde{H}_{50}$ had also to be taken

† Electronic Supplementary Information available. See http://www.rsc.org/suppdata/cp/b1/b102775c/

 DOI: 10.1039/b102775c

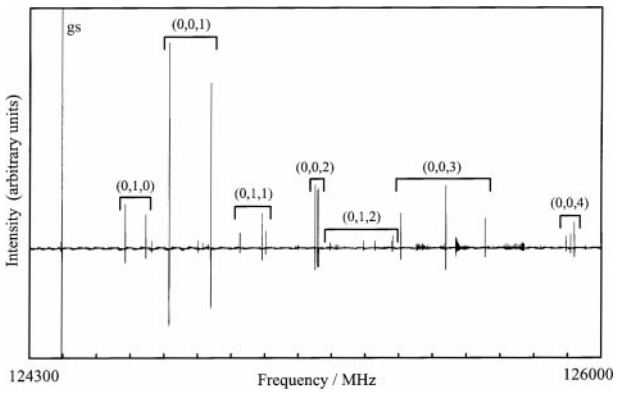

Fig. 1 Recording of a 1.7 GHz wide portion of the rotational spectrum of NCCP in the region of the $J = 23 \leftarrow 22$ transition. Line multiplets belonging to several vibrationally excited states are clearly visible.

into account. The simultaneous analysis of *l*-type and anharmonic resonances has permitted us to reproduce the complex spectral patterns observed within the experimental uncertainties, and, at the same time, to calculate a set of spectroscopic parameters with unambiguous physical meaning.

2 Experimental details

NCCP was produced in a quartz tube by gas-phase pyrolysis of a mixture of methyl cyanide and phosphorus trichloride, as described in ref. 2. The high-temperature reactor ($T \approx 1100\,^{\circ}\mathrm{C}$) was directly connected to the free-space cell of the two mm-wave spectrometers employed and the measurements were carried out by pumping the pyrolysis products continuously through the system. Most of the observed excited state lines were first recorded in the frequency range 118–178 GHz using the broadband mm-wave spectrometer available in Cologne. Later, the frequency range was enlarged in Bologna (from 105 to 220 GHz), where, in addition, the measurements for the (0, 1, 1), (0, 1, 3), and (0, 0, 6) states were performed.

In Cologne, the NCCP rotational spectrum was recorded using the commercial mm-wave spectrometer AM-MSP 3 (Analytik & Meßtechnik GmbH, Chemnitz), whose detailed description is given in ref. 6. Briefly: mm-wave power is generated by a continuous tunable backward wave oscillator tube (BWO) which is phase locked to a reference signal delivered by a synthesized frequency generator operating between 4.0 and 5.4 GHz. The radiation transmitted through the 2.5 m long absorption cell is detected by a silicon Schottky-barrier diode operating at room temperature. Source frequency modulation and 2*f* harmonic detection is employed, so that the second derivative of the actual spectrum profile is recorded. The spectrometer is fully remote controlled *via* a IEEE 488 parallel bus using a personal computer, which also collects and displays the signals produced by the receiver module. Fig. 1 shows a 1.7 GHz wide portion of the rotational spectrum of NCCP, recorded with the Cologne spectrometer, in which a long sequence of lines belonging to many different overtone and combination states is clearly visible.

In Bologna, all the measurements were made using the same Gunn diode, frequency multiplication spectrometer already employed to record the mm-wave spectra in the ground and single excited states of NCCP.[2]

3 Theoretical background

The vibrational energy level structure of linear molecules with more than three atoms is characterized by the presence of states in which different degenerate bending modes can be simultaneously excited, so that they contain several sublevels which differ in the molecular axis component of the vibrational angular momentum. The *l*-type resonance effects which take place among the various *l*-sublevels of a given vibrational state produce a remarkable complexity in the rotational spectrum, which can be greatly enhanced when *l*-dependent anharmonic interactions between different vibrational states are also present. The effective Hamiltonian currently used to analyse the rotational spectra of linear polyatomic molecules in bending states of multiple excitation is that originally proposed by Yamada *et al.*,[7] which summarizes the rovibrational interactions in a very compact form and was successfully applied, for example, by Yamada and co-workers for the analysis of excited state rotational spectra of HC_3N[8] and DC_3N.[9] An exhaustive list of the matrix elements required for the calculation of rovibrational energies for linear polyatomic molecules, including also those necessary to treat anharmonic resonances between different vibrational states, has been recently published by Okabayashi *et al.*[10]

Since the theory is well established, only its essential features are summarized and the matrix elements actually employed for the analysis of the rotational spectrum of NCCP are reported. According to ref. 7, the rovibrational Hamiltonian has been first represented using the unsymmetrized basis functions $|v_4^{l_4}, v_5^{l_5}; J, k\rangle$ each of which is the product of a pair of two-dimensional harmonic wavefunctions and a symmetric-top wavefunction, where $k = l_4 + l_5$. The elements of the Hamiltonian matrix which are diagonal in the vibrational quantum numbers v_t can be expressed employing the simplified notation $|l_4, l_5; J, k\rangle$ and those entirely diagonal in l_t are:

$$\begin{aligned}\langle l_4, l_5; J, k|\hat{H}|l_4, l_5; J, k\rangle &= G_v + x_{L(44)}l_4^2 + x_{L(55)}l_5^2 + x_{L(45)}l_4 l_5 \\ &+ [B_v + d_{JL(44)}l_4^2 + d_{JL(55)}l_5^2 + d_{JL(45)}l_4 l_5] \\ &\times [J(J+1) - k^2] \\ &- [D_v + h_{JL(44)}l_4^2 + h_{JL(55)}l_5^2 + h_{JL(45)}l_4 l_5] \\ &\times [J(J+1) - k^2]^2 \\ &+ H_v[J(J+1) - k^2]^3 \end{aligned} \quad (1)$$

The vibrational *l*-type doubling term ($\Delta l_t = \pm 2$, $\Delta l_{t'} = \mp 2$, $\Delta k = 0$) considered in the present analysis is:

$$\begin{aligned}\langle l_4 \pm 2, l_5 \mp 2; J, k|\hat{H}|l_4, l_5; J, k\rangle &= \tfrac{1}{4}[r_{45} + r_{45J}J(J+1)] \\ &\times \sqrt{(v_4 \mp l_4)(v_4 \pm l_4 + 2)(v_5 \mp l_5 + 2)(v_5 \pm l_5)}\end{aligned} \quad (2)$$

The rotational *l*-type doubling terms ($\Delta l_t = \pm 2$, $\Delta k = \pm 2$) are:

$$\begin{aligned}&\langle l_4 \pm 2, l_5; J, k \pm 2|\hat{H}|l_4, l_s\, J, k\rangle \\ &= \tfrac{1}{4}[q_4 + q_{4J}J(J+1)] \\ &\times \sqrt{(v_4 \mp l_4)(v_4 \pm l_4 + 2)} \\ &\times \sqrt{[J(J+1) - k(k \pm 1)][J(J+1) - (k \pm 1)(k \pm 2)]}\end{aligned} \quad (3)$$

$$\begin{aligned}&\langle l_4, l_5 \pm 2; J, k \pm 2|\hat{H}|l_4, l_5; J, k\rangle \\ &= \tfrac{1}{4}\{q_5 + q_{5J}J(J+1) + q_{5JJ}[J(J+1)]^2\} \\ &\times \sqrt{(v_5 \mp l_5)(v_5 \pm l_5 + 2)} \\ &\times \sqrt{[J(J+1) - k(k \pm 1)][J(J+1) - (k \pm 1)(k \pm 2)]}\end{aligned} \quad (4)$$

As already mentioned in the Introduction, in addition to *l*-type resonance effects, several anharmonic interactions which take origin from the cubic and quintic normal coordinate force constants k_{345}, k_{344}, k_{35555} and k_{34555} have also been considered in the analysis of the measured frequencies. The Hamiltonian for the resonance systems investigated has been constructed in the same way as in ref. 10 and 11, and the following off-diagonal matrix elements have been taken into

account in our calculations:

$$\langle v_3, v_4^{l_4}, v_5^{l_5} | \hat{H}_{30} | v_3 + 1, (v_4 - 1)^{l_4 \pm 1}, (v_5 - 1)^{l_5 \mp 1} \rangle = \frac{\sqrt{2}}{2} [C_{30}^{(345)} + C_{30J}^{(345)} J(J+1)] \times [(v_3 + 1)(v_4 \mp l_4)(v_5 \pm l_5)]^{1/2} \quad (5)$$

$$\langle v_3, v_4^{l_4}, v_5^{l_5} | \hat{H}_{30} | v_3 + 1, (v_4 - 2)^{l_4}, v_5^{l_5} \rangle = \sqrt{2} [C_{30}^{(344)} + C_{30J}^{(344)} J(J+1)] \times [(v_3 + 1)(v_4 - l_4)(v_4 + l_4)]^{1/2} \quad (6)$$

$$\langle v_3, v_4^{l_4}, v_5^{l_5} | \hat{H}_{50} | v_3 + 1, v_4^{l_4}, (v_5 - 4)^{l_5} \rangle = \frac{\sqrt{2}}{2} C_{50}^{(35555)} \times [(v_3 + 1)(v_5 - l_5 - 2)(v_5 + l_5 - 2)(v_5 - l_5)(v_5 + l_5)]^{1/2} \quad (7)$$

$$\langle v_3, v_4^{l_4}, v_5^{l_5} | \hat{H}_{50} | v_3 + 1, (v_4 - 1)^{l_4 \pm 1}, (v_5 - 1)^{l_5 \mp 1} \rangle = \frac{\sqrt{2}}{4} C_{50}^{(34555)} (3v_5 \mp l_5 + 2)[(v_3 + 1)(v_4 \mp l_4)(v_5 \pm l_5)]^{1/2} \quad (8)$$

Eqn. (5)–(7) establish the structure of the polyads which have been analysed for NCCP. The first-order resonance parameters $C_{30}^{(345)}$ and $C_{30}^{(344)}$ arise from the cubic potential terms $\frac{1}{2}k_{345}q_3(q_{4+}q_{5-} + q_{4-}q_{5+})$ and $k_{344}q_3q_{4+}q_{4-}$ respectively, whereas the $C_{50}^{(35555)}$ and $C_{50}^{(34555)}$ coefficients includes the quintic force constants k_{35555} and k_{34555} respectively, together with the related combinations of low-order anharmonic potential constants produced by the perturbation products included in the $\tilde{H}_{50}$ transformed Hamiltonian.[5] The $C_{50}^{(34555)}$ parameter couples the same vibrational states and corresponding sublevels already connected by the first-order resonance coefficient $C_{30}^{(345)}$, but with matrix elements which have a different l_5 dependence. It was introduced in our model to reproduce within experimental accuracy the lines observed for the (0, 1, 2) and (0, 1, 3) bending combination states, where many sublevels, characterized by different l_5 values, are involved in the resonance primarily produced by $C_{30}^{(345)}$.

The C_{30} coefficients are directly related to the corresponding normal coordinate cubic force constants through the expression:

$$k_{3tt'} = 4C_{30}^{(3tt')} \quad (9)$$

The resulting energy matrix has been then factorized in symmetric and antisymmetric blocks adopting the following Wang-type linear combinations of rovibrational wavefunctions:[8,9]

$$|v_4^{l_4}, v_5^{l_5}; J, k\rangle_\pm = \frac{1}{\sqrt{2}} [|v_4^{l_4}, v_5^{l_5}; J, k\rangle \pm |v_4^{-l_4}, v_5^{-l_5}; J, -k\rangle] \quad (10)$$

$$|v_4^0, v_5^0; J, 0\rangle_+ = |v_4^0, v_5^0; J, 0\rangle \quad (11)$$

where expression (11) is used when a given state has all the l_t quantum numbers equal to zero. When two different bending modes v_t and $v_{t'}$ are simultaneously excited, the wavefunctions are expressed by linear combinations of $(v_t + 1)$ $(v_{t'} + 1)$ basis functions $|v_t^{l_t}, v_{t'}^{l_{t'}}; J, k\rangle$. For example, the basis functions for the (0, 1, 3) state may be generated from eqn. (10) in which $l_4 = \pm 1$ and l_5 ranges from 3 to -3 in steps of two; the eight symmetrized wavefunctions obtained are labelled according to their k values in the following way: $4^\pm$, $2^\pm$, $0^\pm$ and $-2^\pm$, where the plus or minus superscript indicates whether the sum or the difference is taken in the linear combination.

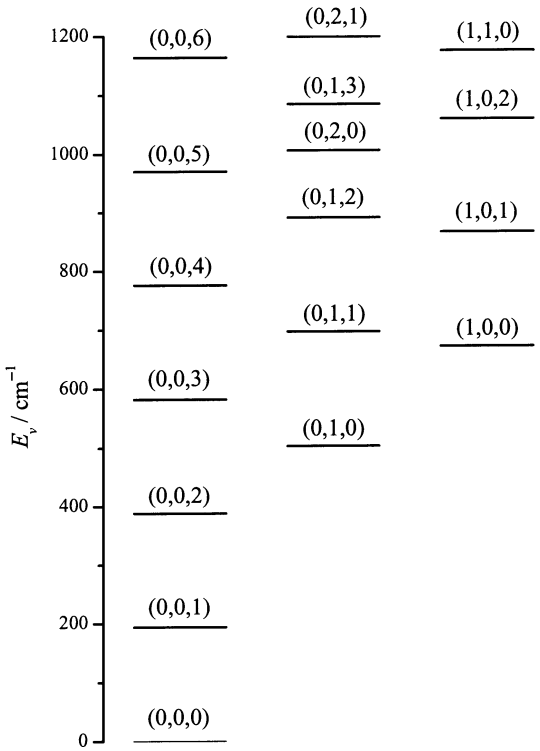

Fig. 2 Approximate vibrational energy level diagram of NCCP up to 1200 cm^{-1}.

4 Observed spectra and analyses

The approximate vibrational energy level diagram of NCCP up to 1200 cm^{-1} is illustrated in Fig. 2. Since no infrared spectrum has been observed till now for this molecule, the position of the levels was determined using the *ab initio* computed harmonic wavenumbers reported in ref. 2. The diagram includes 16 excited vibrational states, 3 of which ((1, 0, 0), (0, 1, 0) and (0, 0, 1)) had been already investigated by mm-wave and submm-wave spectroscopy in previous works,[2,3] while the remaining 13, corresponding to overtones and combinations of the fundamental levels, are the object of the present study. All the new states investigated involve the excitation of at least one bending mode, so that multiplets of rotational lines were observed for each $J + 1 \leftarrow J$ transition, owing to the presence of different sublevels. An example is given in Fig. 3, which shows the five lines recorded for the $J = 20 \leftarrow 19$ transition of the (0, 0, 6) state, which lies $\approx$1160 cm^{-1} above the ground state.

In the first stage of the analysis, effective polynomial fits were performed for the transition frequencies assigned to each

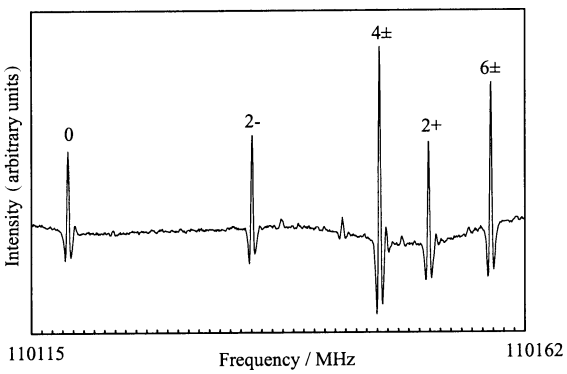

Fig. 3 Recording of the $J = 20 \leftarrow 19$ rotational transition of NCCP in the vibrationally excited state (0, 0, 6).

Table 1 Spectroscopic constants determined for the (0, 0, 2) and (0, 0, 3) vibrationally excited states of NCCP.[a] Standard errors in units of the last quoted digit are given in parentheses for the fitted constants

	(0, 0, 2)	(0, 0, 3)	
B_v	2720.973 18(13)	2729.176 28(14)	MHz
$d_{JL(55)}$	16.262(31)	15.512(25)	kHz
D_v	0.219 163(58)	0.228 497(52)	kHz
$h_{JL(55)}$	0.0489[b]	0.0489[b]	Hz
H_v	0.036 98[b]	0.049 87[b]	mHz
q_5	2.705 21[b]	2.711 22(12)	MHz
q_{5J}	−4.389[b]	−4.510(68)	Hz
q_{5JJ}	9.33[b]	9.33[b]	μHz
$x_{L(55)}$	25.522(11)	25.157(38)	GHz
σ	11.7	11.2	kHz
no. of lines	39	37	
J range	19–37	19–37	

[a] Vibrational states are labelled by (v_3, v_4, v_5). [b] Derived value, see Section 4.

sublevel using the standard expression for linear molecules in Σ states:

$$\nu = 2B_v(J+1) - 4D_v(J+1)^3 + 2H_v(3J^2+6J+4)(J+1)^3 \quad (12)$$

Generally, l-type resonance effects produce anomalous values for the effective centrifugal distortion constants, while the presence of anharmonic interactions is mainly revealed by irregular changes in the fitted rotational constants.

This latter effect was clearly observed for the 0^+ component of the bending combination state (0, 1, 1), and it can be explained in terms of an anharmonic interaction with the nearby stretching state (1, 0, 0) through the k_{345} normal coordinate cubic force constant. A careful check of the measured absorption frequencies showed that the $l = 0$ sublevels of (0, 2, 0) and (0, 0, 4) are also weakly coupled to (1, 0, 0) through cubic and quintic anharmonic terms respectively. Therefore, the first resonance system of NCCP consists of the four states (1, 0, 0), (0, 1, 1), (0, 2, 0) and (0, 0, 4), whose rotational spectra were consequently analysed simultaneously.

The adopted interaction scheme led us to consider two further resonance systems. The second polyad can be constructed by addition of one quantum of v_5 or v_4 to the levels of the first resonance system, and it therefore includes the investigated states (1, 0, 1), (0, 1, 2), (0, 2, 1), (0, 0, 5) and (1, 1, 0). The third polyad contains the levels which are derived

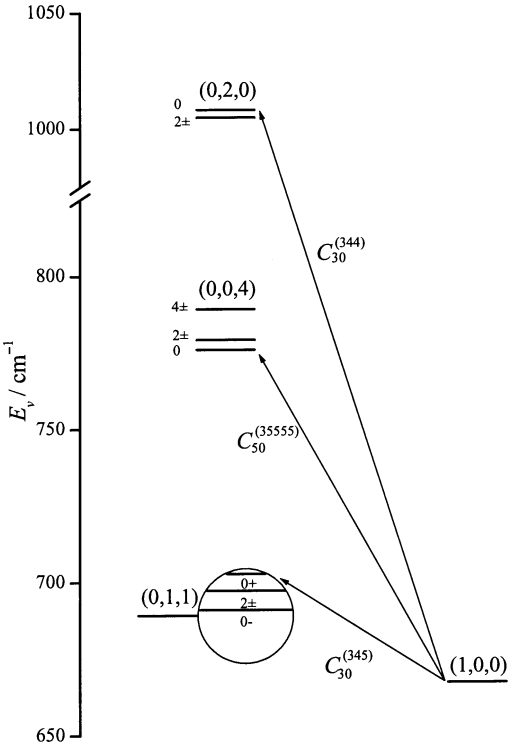

Fig. 4 Vibrational energy level diagram for the first resonance system of NCCP. Arrows indicate the anharmonic interactions taken into account.

from the first resonance system upon addition of two quanta of the lowest bending v_5, and thus it includes the observed states (1, 0, 2), (0, 1, 3) and (0, 0, 6). The states (0, 0, 2) and (0, 0, 3) appear to be the only ones not involved in resonances, and so they were treated as isolated states.

The more than 600 transition frequencies measured in the course of the present investigation were analysed performing five independent least-squares fits: for (0, 0, 2), for (0, 0, 3), and for the first, second, and third resonance systems, respectively. However, several constraints had to be adopted in each calculation. These assumptions were very often based on the results obtained from some different analysis, and this produced a certain degree of mutual dependence between the values determined in the various least-squares calculations, which were therefore repeated cyclically, with up-to-date constraints, in order to achieve a high degree of consistency between the

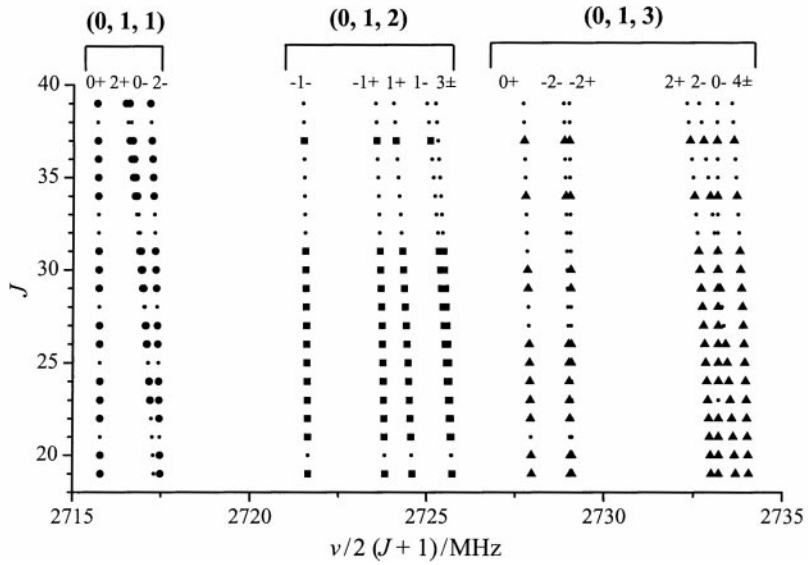

Fig. 5 Reduced transition frequencies for the (0, 1, 1), (0, 1, 2) and (0, 1, 3) vibrational states of NCCP. Solid symbols identify the measured frequencies.

parameters obtained from the five independent fits. Whenever possible, a linear dependence on the vibrational quantum numbers has been assumed to extrapolate the values of the constrained constants. The final results determined with this converging procedure are those reported in the forthcoming tables, and some details concerning the single analyses performed are presented in the following subsections. The complete list of fitted transition frequencies is available as supplementary material.†

4.1 Analysis of isolated states: (0, 0, 2) and (0, 0, 3)

The rotational spectra of the apparently unperturbed (0, 0, 2) and (0, 0, 3) states have been identified and assigned in a straightforward way. 39 and 37 rotational transitions were recorded for (0, 0, 2) and (0, 0, 3) respectively, from $J = 19$ to $J = 37$. The experimental frequencies were analysed using eqn. (1) and (4), which take into account the effects due to rotational l-type resonances. The parameters obtained from the two least-squares fits are listed in Table 1. The l-doubling constants q_5 and q_{5J} of the (0, 0, 2) state are indeterminable in an independent fit, and so they were held constrained to the values calculated by linear interpolation of the results obtained for the (0, 0, 1)[3] and (0, 0, 3) states.

4.2 Analysis of the first resonance system: [(1, 0, 0) ~ (0, 1, 1) ~ (0, 2, 0) ~ (0, 0, 4)]

Fig. 4 shows the vibrational energy level diagram for the first resonance system of NCCP. It contains four vibrational states and it is very similar to the one already analysed for HC_3P,[4] the main difference being the inversion which occurs between the low energy stretching state and the nearby bending combination state. The strongest anharmonic interaction is produced by the cubic potential constant k_{345} which couples the (1, 0, 0) and (0, 1, 1) states. This resonance was clearly revealed by the results obtained from effective fits performed separately for the observed transition frequencies of each sublevel of the (0, 1, 1) bending combination state. Whereas three components of the quadruplet (0^-, 2^+ and 2^-) are characterized by B_v constants very close to the predicted unperturbed value of 2717.52 MHz, a B_v constant 1.7 MHz smaller was obtained for the 0^+ sublevel. The anomalous low-frequency displacement of the lines belonging to the 0^+ sublevel of (0, 1, 1) is apparent in Fig. 5, where the reduced transition frequencies $\nu_{red} = \nu_{obs}/2(J + 1)$ for several bending combination states are plotted *vs.* J for different J values. In addition, the analysis of the mm-wave lines previously measured for the (1, 0, 0) state[2] yielded an effective B_v constant 1.9 MHz greater than that predicted using the *ab initio* computed value of the α_3 vibration–rotation coupling constant. Both these anomalies can be easily explained assuming an anharmonic interaction between the (1, 0, 0) and (0, 1, 1) states.

A weaker perturbation was also detected in the spectrum of the (0, 2, 0) state, whose $l_4 = 0$ sublevel has an effective B_v constant which is ≈400 kHz smaller than that observed for the $l_4 = 2$ sublevels. This suggested to us the presence of a weak Fermi resonance between (1, 0, 0) and (0, 2, 0). The theoretical calculations reported in ref. 2 predict a purely harmonic energy difference of 334 cm^{-1} between (0, 2, 0) and (1, 0, 0), with $k_{344} = 39.7$ cm^{-1}. These values can account for a 100 kHz decreasing of the effective value of B_v for the (0, 2, 0) $l_4 = 0$ sublevel, and so further contributions coming from the rotational dependence of the Fermi resonance (the $C_{30J}^{(344)}$ parameter of eqn. (6)) and/or from the $d_{JL(44)}$ term should be also considered to reproduce correctly the spectrum observed for the (0, 2, 0) state. As far as the (0, 0, 4) state is concerned, a careful inspection of the transition frequencies measured showed that they could not be satisfactorily fitted by considering only l-type resonance effects, but it was also necessary to assume a certain degree of mixing of the 0^+ sublevel with a vibrational state characterized by a lower rotational constant, and the final analysis was therefore performed also taking into account the quintic anharmonic term which connects (1, 0, 0) with (0, 0, 4).

A total of 174 lines belonging to 13 l-sublevels of the 4 interacting states were simultaneously analysed using a non-linear, least-squares fitting procedure. The 29 transition frequencies analysed for the (1, 0, 0) state come entirely from previous studies. In particular, we used the 16 mm-wave transitions already reported in ref. 2, and 13 still unpublished submm-wave lines which were recorded in the frequency range from 490 to 770 GHz during a previous investigation of the submm-wave spectrum of NCCP.[3] The spectroscopic parameters obtained from the analysis of the first resonance system are collected in Table 2.

For the strongest anharmonic interaction it was possible to fit simultaneously both the off-diagonal term $C_{30}^{(345)}$ and the

Table 2 Spectroscopic constants determined for the vibrationally excited states of the first resonance system of NCCP.[a] Standard errors in units of the last quoted digit are given in parentheses for the fitted constants

	(1, 0, 0)	(0, 1, 1)	(0, 2, 0)	(0, 0, 4)	
ΔG_v[b]	0.0	17.241(31)	334.0[c]	104.0[c]	cm^{-1}
B_v	2699.788 96(22)	2717.540 756(98)	2713.960 983(94)	2737.354 71(11)	MHz
$d_{JL(45)}$	—	8.61(10)	—	—	kHz
$d_{JL(55)}$	—	17.973[c]	—	14.7874(58)	kHz
D_v	0.200 859(49)	0.213 300(41)	0.207 447(42)	0.237 909(51)	kHz
$h_{JL(55)}$	—	0.0489[c]	—	0.0489[c]	Hz
H_v	0.012 55(96)	0.026 02[c]	0.015 06[c]	0.062 76[c]	mHz
q_4	—	1.323 07[c]	1.323 07[c]	—	MHz
q_{4J}	—	−0.2577[c]	−0.2577[c]	—	Hz
q_5	—	2.699 19[c]	—	2.717 66[c]	MHz
q_{5J}	—	−4.2685[c]	—	−4.544[c]	Hz
q_{5JJ}	—	9.33[c]	—	9.33[c]	μHz
$x_{L(44)}$	—	−8.216[c]	−8.216(57)	—	GHz
$x_{L(45)}$	—	16.189(26)	—	—	GHz
$x_{L(55)}$	—	25.694[c]	—	24.7835(58)	GHz
r_{45}	—	−16.764(52)	—	—	GHz
no. of lines	29	54	41	50	
J range	19–141	19–39	19–39	19–37	

$C_{30}^{(345)} = 3.7029(51)$ cm^{-1} $\quad C_{30J}^{(344)} = -0.644\,20(24)$ MHz
$C_{50}^{(34555)} = -0.0714$[c] cm^{-1} $\quad C_{50}^{(35555)} = 0.2160(28)$ cm^{-1}
$C_{30}^{(344)} = 9.875$[c] cm^{-1} $\quad \sigma = 11.7$ kHz

[a] Vibrational states are labelled by (v_3, v_4, v_5). [b] Vibrational energy relative to the (1, 0, 0) state. [c] Derived value, see Section 4.

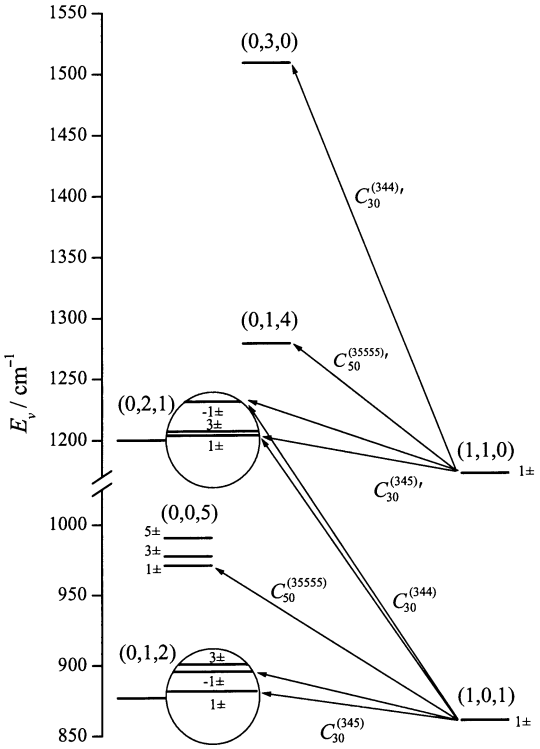

Fig. 6 Vibrational energy level diagram for the second resonance system of NCCP. Arrows indicate the anharmonic interactions taken into account. No lines were recorded for the (0, 3, 0) and (0, 1, 4) states.

vibrational energy difference $G_v(0, 1, 1) - G_v(1, 0, 0)$. The fitted values, $C_{30}^{(345)} = 3.70$ cm^{-1} and $\Delta G_v = 17.2$ cm^{-1}, compare favourably with the corresponding theoretical estimates, which are $C_{30}^{(345)} = 3.41$ cm^{-1} and $\omega_4 + \omega_5 - \omega_3 = 24$ cm^{-1}.[2] As for the resonance between (1, 0, 0) and (0, 2, 0), too many parameters can contribute to the observed low-frequency displacement of the lines belonging to the $l_4 = 0$ sublevel, and some assumption had to be made. As already done for HC_3P,[4] the vibrational energy difference $G_v(0, 2, 0) - G_v(1, 0, 0)$ and the main off-diagonal term $C_{30}^{(344)}$ were both held fixed to the corresponding *ab initio* computed values,[2] while the $C_{30J}^{(344)}$ parameter was released in the least-squares fit. This procedure allowed us to reproduce well the experimental frequencies of the (0, 2, 0) state, avoiding at the same time convergence towards an unreasonably large value of the cubic $C_{30}^{(344)}$ term. The simultaneous adjustment of $C_{30J}^{(344)}$ and $d_{JL(44)}$ produced a completely indeterminate value of the latter constant, which was therefore assumed equal to zero.

Finally, for the very weak resonance between (1, 0, 0) and (0, 0, 4), the vibrational energy difference was held fixed to the value calculated using *ab initio* computed harmonic wavenumbers, while the off-diagonal quintic term $C_{50}^{(35555)}$ was fitted to the experimental data. It is to be noted that in the present case only the absolute values of the off-diagonal elements of the tetrad can be determined, and we have assumed conventionally a positive sign for the leading terms $C_{30}^{(345)}$, $C_{30}^{(344)}$ and $C_{50}^{(35555)}$.

Further parameters held fixed in this analysis were derived from the results of least-squares fittings carried out in the present or previous works[3] for other vibrational states. It is to be noted that the high-J transition frequencies available for the (1, 0, 0) state allowed us to obtain also the sextic centrifugal distortion constant for this level, whose fitted value is quite close to that determined previously for the ground state.[3]

4.3 Analysis of the second resonance system: [(1, 0, 1) ~ (0, 1, 2) ~ (0, 2, 1) ~ (0, 0, 5) ~ (1, 1, 0)]

Two further tetrads can be constructed by addition of one quantum of the v_5 or v_4 bending modes to the members of the first resonance system. These are (1, 0, 1) ~ (0, 1, 2) ~ (0, 2, 1) ~ (0, 0, 5) and (1, 1, 0) ~ (0, 2, 1) ~ (0, 3, 0) ~ (0, 1, 4). Actually, these two polyads are not independent, since both include the common state (0, 2, 1), and they constitute the second resonance system of NCCP, whose vibrational energy level diagram is illustrated in Fig. 6. No lines were recorded for the two vibrational states which lie above 1200 cm^{-1}, (0, 1, 4) and (0, 3, 0) (directly connected with (1, 1, 0) through $C_{50}^{(35555)\prime}$ and $C_{30}^{(344)\prime}$ respectively), but they were included in the calculation to reduce systematic errors in the fitted constants. The corresponding spectroscopic parameters and resonance terms were assumed or extrapolated from the spectra already analysed, and they are listed in the supplementary

Table 3 Spectroscopic constants determined for the vibrationally excited states of the second resonance system of NCCP.[a] Standard errors in units of the last quoted digit are given in parentheses for the fitted constants

	(1, 0, 1)	(0, 1, 2)	(0, 2, 1)	(1, 1, 0)	(0, 0, 5)	
ΔG_v[b]	0.0	10.799(55)	334.0[c]	313.1581(97)	104.0[c]	cm^{-1}
B_v	2707.897 19(52)	2725.808 25(15)	2722.302 44(15)	2704.500 16(56)	2745.510 48(16)	MHz
$d_{JL(45)}$	—	8.61[c]	8.61[c]	—	—	kHz
$d_{JL(55)}$	21.144[c]	17.223[c]	17.012[c]	—	14.1575(52)	kHz
D_v	0.208 44(32)	0.222 77(11)	0.216 207(46)	0.205 197(78)	0.247 417(47)	kHz
$h_{JL(55)}$	0.0489[c]	0.0489[c]	0.0489[c]	—	0.0489[c]	Hz
H_v	0.025 28[c]	0.038 91[c]	0.027 95[c]	0.014 32[c]	0.075 65[c]	mHz
q_4	—	1.347 63(22)	1.323 07[c]	1.366 39(12)	—	MHz
q_{4J}	—	−0.2577[c]	−0.2577[c]	−0.2577[c]	—	Hz
q_5	2.712 61(20)	2.705 21[c]	2.720 38(18)	—	2.724 078(84)	MHz
q_{5J}	−4.2685[c]	−4.389[c]	−4.2685[c]	—	−4.576(46)	Hz
q_{5JJ}	9.33[c]	9.33[c]	9.33[c]	—	9.33[c]	μHz
$x_{L(44)}$	—	−8.216[c]	−7.567(65)	−8.216[c]	—	GHz
$x_{L(45)}$	—	15.798(99)	16.3109(27)	—	—	GHz
$x_{L(55)}$	27.146[c]	25.329(19)	25.887[c]	—	24.465(17)	GHz
r_{45}	—	−15.85(17)	−16.182(30)	—	—	GHz
no. of lines	26	67	47	26	55	
J range	19–37	19–37	19–37	19–37	19–37	
		$C_{30}^{(345)} = 3.7413(34)$ cm^{-1}		$C_{50}^{(35555)} = 0.2316(15)$ cm^{-1}		
		$C_{50}^{(34555)} = -0.0827(25)$ cm^{-1}		$C_{30}^{(345)\prime} = 3.7029$[d] cm^{-1}		
		$C_{30}^{(344)} = 9.875$[c] cm^{-1}		$C_{50}^{(34555)\prime} = -0.0714$[d] cm^{-1}		
		$C_{30J} = -0.747\,26(61)$ MHz		$\sigma = 11.6$ kHz		

[a] Vibrational states are labelled by (v_3, v_4, v_5). [b] Vibrational energy relative to the (1, 0, 1) state. [c] Derived value, see Section 4. [d] Anharmonic coefficients related to the (1, 1, 0)–(0, 2, 1) interaction. Values assumed from the first resonance system.

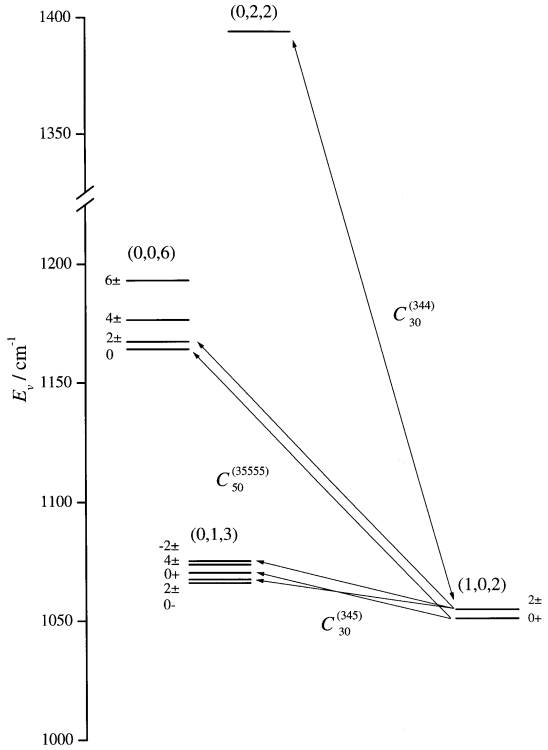

Fig. 7 Vibrational energy level diagram for the third resonance system of NCCP. Arrows indicate the anharmonic interactions taken into account. No lines were recorded for the (0, 2, 2) state.

material. Two strong anharmonic interactions are included in the second resonance system: the one which couples the (1, 0, 1) state with (0, 1, 2), and the one between (1, 1, 0) and (0, 2, 1).

Effective fittings performed using eqn. (12) showed that both components of the (1, 0, 1) doublets undergo a frequency displacement corresponding to an effective rotational constant about 3.8 MHz greater than the extrapolated, unperturbed value. This means that the effect of the anharmonic interaction due to k_{345} is nearly twice as large as that observed in the first resonance system. On the contrary, the position of the (1, 1, 0) doublets corresponds to an effective rotational constant 2.3 MHz greater than the predicted, unperturbed value, and this indicates that the resonance between (1, 1, 0) and (0, 2, 1) is only slightly stronger than that between (1, 0, 0) and (0, 1, 1).

A total of 221 transition frequencies belonging to 22 different l-sublevels were analysed for the second resonance system. The same scheme of anharmonic interactions employed for the first tetrad was used, but the increased number of l-sublevels included in the calculation produced a considerable enhancement of correlation between the parameters, and thus several constraints had to be applied in order to avoid an excessive instability of the non-linear least-squares fitting procedure. The values obtained for the fitted constants and the constraints adopted are gathered in Table 3. For the very strong resonance between the (1, 0, 1) and (0, 1, 2) states it was possible to fit both the off-diagonal coupling term $C_{30}^{(345)}$ and the corresponding vibrational energy difference, but in the case of the weaker interaction between (1, 1, 0) and (0, 2, 1), the increased correlation effects led us to assume the coupling constant $C_{30}^{(345)'}$ from the first resonance system, and only the energy difference $G_v(0, 2, 1) - G_v(1, 1, 0)$ was fitted to the experimental data. The two remaining anharmonic interactions which involve observed states (namely the one between (1, 0, 1) and (0, 0, 5), and the one between (1, 0, 1) and (0, 2, 1)) were treated exactly as in the first tetrad.

In the initial stage of the calculation, the same parameters already used to analyse the first resonance system were employed, and a fairly good, but not completely satisfactory fit was obtained ($\sigma = 28$ kHz), since deviations up to 160 kHz were observed for the lines of the (0, 1, 2) state. Several high-order, l-type resonance parameters were then released in the fit, such as r_{45J}, q_{455} and u_{55},[10] but none of them allowed for a significant reduction of the least-squares residuals. This suggested the observed anomalies to arise from high-order anharmonic terms able to change slightly the strength of the resonance between the sublevels of the (1, 0, 1) and (0, 1, 2) states, depending on the l_5 values involved, and a clear decreasing of the standard deviation (down to $\sigma = 12$ kHz) was finally obtained when the high-order parameter $C_{50}^{(34555)}$ was set free in the least-squares calculation.

4.4 Analysis of the third resonance system: [(1, 0, 2) ~ (0, 1, 3) ~ (0, 0, 6)]

The third resonance system considered in the present work includes the states derived from those of the first resonance

Table 4 Spectroscopic constants determined for the vibrationally excited states of the third resonance system of NCCP.[a] Standard errors in units of the last quoted digit are given in parentheses for the fitted constants

	(1, 0, 2)	(0, 1, 3)	(0, 0, 6)	
ΔG_v [b]	0.0	4.9182(67)	104.0[c]	cm^{-1}
B_v	2715.960 29(31)	2734.046 66(16)	2753.645 56(18)	MHz
$d_{JL(45)}$	—	8.61[c]	—	kHz
$d_{JL(55)}$	20.397(59)	16.472(16)	13.5886(78)	kHz
D_v	0.217 63(13)	0.231 995(57)	0.257 030(63)	kHz
$h_{JL(55)}$	0.0489[c]	0.0489[c]	0.0489(35)	Hz
H_v	0.038 17[c]	0.051 80[c]	0.088 54[c]	mHz
q_4	—	1.4123(34)	—	MHz
q_{4J}	—	−0.2577[c]	—	Hz
q_5	2.718 64[c]	2.711 22[c]	2.730 52[c]	MHz
q_{5J}	−4.389[c]	−4.578[c]	−4.612[c]	Hz
q_{5JJ}	9.33[c]	9.33[c]	9.33[c]	μHz
$x_{L(44)}$	—	−8.216[c]	—	GHz
$x_{L(45)}$	—	15.702(31)	—	GHz
$x_{L(55)}$	26.7943(68)	24.8680(71)	24.2427(21)	GHz
r_{45}	—	−15.828(40)	—	GHz
no. of lines	39	84	44	
J range	19–37	19–37	19–37	
	$C_{30}^{(345)} = 3.8721(34)$ cm^{-1}		$C_{50}^{(35555)} = 0.250\,14(37)$ cm^{-1}	
	$C_{50}^{(34555)} = -0.093\,99(71)$ cm^{-1}		$\sigma = 11.8$ kHz	

[a] Vibrational states are labelled by (v_3, v_4, v_5). [b] Vibrational energy relative to the (1, 0, 2) state. [c] Derived value, see Section 4.

system upon addition of two quanta of the lowest bending mode v_5. The corresponding energy level diagram is shown in Fig. 7. We have observed rotational transitions for three of these states, namely (1, 0, 2), (0, 1, 3) and (0, 0, 6), but the so far unobserved state (0, 2, 2) (directly connected with (1, 0, 2) through k_{344}) was also included in the analysed polyad. The assumed spectroscopic parameters and resonance terms are reported in the supplementary material. The progressive strengthening of the main resonance produced by excitation of the lowest bending mode was confirmed also in the third resonance system, since the effective B_v constant for the (1, 0, 2) state is about 6.2 MHz greater than the corresponding unperturbed value. This trend is also well illustrated in Fig. 5, where the progressive low-frequency displacement of the most perturbed lines belonging to the different l-sublevels of the (0, 1, 1), (0, 1, 2) and (0, 1, 3) states is manifest.

A total number of 167 measured transition frequencies, belonging to 18 l-sublevels of 3 different vibrational states, was analysed for the third resonance system of NCCP. At the beginning, the same spectroscopic constants already used for the analysis of the second resonance system were employed, but excellent results were only obtained when two more parameters were set free, that are the $d_{JL(55)}$ constant for the (1, 0, 2) state, and the high-order l-type resonance parameter $h_{JL(55)}$ for the highly excited overtone state (0, 0, 6). The considerable strengthening of the resonance due to the $C_{30}^{(345)}$ coupling term produced also an increasing importance of the high-order $C_{50}^{(34555)}$ term, which was in fact determined with better precision. The complete set of spectroscopic constants which were used to reproduce the measured transition frequencies for the third resonance system of NCCP are collected in Table 4.

5 Conclusion

This paper presents an extensive study of the rotational spectra of NCCP in vibrationally excited states up to 1200 cm^{-1}. Several resonance systems have been identified, and the interacting levels have been analysed simultaneously taking into account both l-type and anharmonic resonance effects in order to calculate spectroscopic parameters with a clear physical meaning. Only 2 vibrational states out of 13 studied could be analysed satisfactorily as isolated states, and several anharmonic interactions, some of which were very weak, had to be taken into account for all other states to reproduce the measured transition frequencies within experimental accuracy. This can be explained by considering that typically anharmonic resonances act in different ways on the various l-sublevels of a given bending vibrational state, so that noticeable changes in the splittings observed between lines belonging to different l-sublevels are produced. This effect cannot be easily absorbed by the spectroscopic parameters involved in l-type resonances, and so even very weak anharmonic interactions must be accounted for to fit satisfactorily the multiplets of lines produced by bending mode excitation.

The analysis of the first resonance system in which the (1, 0, 0) stretching state is strongly coupled with (0, 1, 1), and to a lesser extent with (0, 2, 0) and (0, 0, 4), allowed us to explain the anomalous, effective value previously calculated for the α_3 vibration–rotation coupling constant.[2] The experimental, unperturbed α_3 value of 4.69 MHz is now in good agreement with the *ab initio* estimate of 4.48 MHz,[2] and a similarly good agreement has also been obtained for the normal coordinate cubic force constant k_{345}, whose experimental value of 14.8 cm^{-1} is near to the theoretical prediction of 13.6 cm^{-1}. The anharmonic interactions analysed in the present work have also yielded experimental estimates of the quintic coefficients $C_{50}^{(35555)}$ and $C_{50}^{(34555)}$, whose values seem to be of reasonable order of magnitude. Let us write symbolically the terms of the rovibrational Hamiltonian $\hat{H}_{mn}$ as:

$$\hat{H}_{mn} = C_{mn}\hat{\mathcal{P}}^m\hat{J}^n \tag{13}$$

where C_{mn} is a coefficient, m the sum of the powers of the vibrational operators, and n the sum of the powers of the rotational operators. According to Aliev and Watson[5] the order of magnitude of the coefficient C_{mn} is estimated to be:

$$C_{mn} \approx \kappa^{m+2n-2}\omega_{vib} \tag{14}$$

where an approximate value of $\kappa \approx 0.1$ can be adopted for most vibrational problems. The ratio between quintic and cubic potential terms is therefore given by:

$$\frac{C_{50}}{C_{30}} \approx \frac{\kappa^3}{\kappa^1} \approx 10^{-2} \tag{15}$$

The values obtained for the two C_{50} terms fitted are of the order of 0.1 cm^{-1}, and they are therefore consistent with the estimated order of magnitude. The fitted value of the $C_{30J}^{(344)}$ parameter has also the order of magnitude expected for the coefficient which gives the J dependence of an off-diagonal element of a first-order anharmonic interaction.[12]

The increasing strength of the resonance produced by k_{345}, observed as a consequence of progressive excitation of the v_5 mode, is essentially due to the anharmonic contributions to the interacting vibrational states, which make them progressively closer. The experimental energy differences calculated by our analyses are in fact 17.24 cm^{-1} between (1, 0, 0) and (0, 1, 1), 10.80 cm^{-1} between (1, 0, 1) and (0, 1, 2) and 4.92 cm^{-1} between (1, 0, 2) and (0, 1, 3). A careful inspection of the final results reported in Tables 1–4 shows that typically the spectroscopic constants which appear in the diagonal elements of the rovibrational energy matrices exhibit a regular, nearly linear dependence on the vibrational quantum numbers, while less regular trends characterize the parameters involved in the off-diagonal elements, mainly because they are more easily affected by instabilities produced by correlation effects. No important anomaly is however apparent in the obtained results, even if systematic errors are surely present, owing to the assumptions made from *ab initio* calculations[2] and the need to truncate the energy matrices related to the second and third resonance systems.

The spectroscopic parameters obtained in the present and previous works[2,3] allow for accurate predictions for the rotational energies of a plethora of vibrationally excited states, and this can be very useful for the analysis of the high-resolution infrared spectra of this molecule, whose detection may however be difficult, because very low intensities are theoretically predicted for the fundamental bands of NCCP.[13]

Acknowledgements

The authors wish to thank the referee who pointed out that an incorrect equation was formulated in the original version of the article.

We are grateful to Prof. Manfred Winnewisser and Dr Stefan Klee (Physikalisch-Chemisches Institut, Justus Liebig Universität Gießen, Germany) for providing the tube furnace used in Cologne.

L. B. thanks the members of the I. Physikalische Institut for hospitality during his three-month stay in Cologne. He also expresses appreciation for all the efforts of the administration of the Universität zu Köln toward having his subsistence allowance, granted by the Deutsche Forschungsgemeinschaft (DFG).

References

1 T. A. Cooper, H. W. Kroto, J. F. Nixon and O. Ohashi, *J. Chem. Soc., Chem. Commun.*, 1980, 333.
2 L. Bizzocchi, C. Degli Esposti and P. Botschwina, *J. Chem. Phys.*, 2000, **113**, 1465.

3 L. Bizzocchi, S. Thorwirth, H. S. P. Müller, F. Lewen and G. Winnewisser, *J. Mol. Spectrosc.*, 2001, **205**, 110.
4 L. Bizzocchi, C. Degli Esposti, L. Dore and G. Cazzoli, *J. Mol. Spectrosc.*, 2001, **205**, 164.
5 M. R. Aliev and J. K. G. Watson, in *Molecular Spectroscopy: Modern Research*, ed. K. Narahari Rao, Academic Press, New York, 1985, vol. III, pp. 1–67.
6 M. Winnewisser, H. Lichau and F. Wolf, *J. Mol. Spectrosc.*, 2000, **202**, 155.
7 K. M. T. Yamada, F. W. Birss and M. R. Aliev, *J. Mol. Spectrosc.*, 1985, **112**, 347.
8 K. M. T. Yamada and R. A. Creswell, *J. Mol. Spectrosc.*, 1986, **116**, 404.
9 G. M. Plummer, D. Mauer, K. M. T. Yamada and K. Möller, *J. Mol. Spectrosc.*, 1988, **130**, 407.
10 T. Okabayashi, K. Tanaka and F. Tanaka, *J. Mol. Spectrosc.*, 1999, **195**, 22.
11 G. Wagner, B. P. Winnewisser, M. Winnewisser and K. Sarka, *J. Mol. Spectrosc.*, 1993, **162**, 82.
12 J. K. G. Watson, *J. Mol. Spectrosc.*, 1988, **132**, 477.
13 O. Kwon and M. L. McKee, *J. Phys. Chem. A*, 2001, **105**, 478.